Exploring and applying sparse regression in admittance-based TPA methods

D. Ocepek [1], **F. Trainotti** [2], **J. Korbar** [1], **D. J. Rixen** [2], **M. Boltežar** [1], **G. Čepon** [1]
[1] University of Ljubljana, Faculty of Mechanical Engineering,
Laboratory for Dynamics of Machines and Structures,
Aškerčeva 6, 1000 Ljubljana, Slovenia

[2] Technical University of Munich, School of Engineering and Design, Chair of Applied Mechanics,
Boltzmannstr. 15, 85748 Garching, Germany

Abstract
This study investigates the use of sparse regression, specifically LASSO (least absolute shrinkage and selection operator), in admittance-based transfer path analysis (TPA) to identify critical transmission paths for sound and vibration propagation in assembled products. Application of TPA methods notoriously requires careful interface modeling in terms of interface degrees of freedom (DoFs) to avoid redundancy and error amplification in the estimated set of forces that replicate assembly's operational response. LASSO sheds light on the selection of the significant interface DoFs by promoting sparsity in the set of DoFs proposed by experimentalist. Case studies on single- and multi-point interfaces provide insights into the implementation and application of the sparse regression for use in inverse problem of TPA methods.

1 Introduction

When determining critical paths for transmission of sound and vibration in assembled products, transfer path analysis (TPA) is a reliable and effective tool [1, 2]. TPA represents a source with a set of forces that replicates the operational response, initially generated by the vibrating source. Using a component-based TPA family one can identify a set of equivalent forces that are inherent property of the source and are valid for any assembly with a modified receiver [2]. The indirect determination of the forces at the interface degrees of freedom (DoFs) is commonly performed using an inverse procedure directly in-situ [3], where equivalent forces are estimated from the admittance of the transfer paths and operational responses of the receiver in an assembly. Interface DoFs can be interpreted as the transfer paths from the source to receiver. That means the experimentalist must be able to identify, control, and observe all significant interface DoFs when estimating admittance of the transfer paths, otherwise, equivalent forces are a property of the assembly (not the source), and their transferability to modified assemblies is limited [4].

Modeling too many interface DoFs can result in redundancy and consequently bad conditioning of the admittance matrix. Ill-conditioning combined with inevitably present measurement errors can lead to a high error amplification in the equivalent forces, thus limiting their transferability[1]. On the other hand, modeling to few interface DoFs can again significantly deteriorate the transferability of the equivalent forces[2]. Recently, virtual point transformation (VPT) [6] has been proposed to model the interface where interface DoFs (rigid or flexible) are selected manually by the experimentalist to avoid redundancy yet retain the full controllability of the interface [7]. However, the manual nature of virtual DoF selection proves to be challenging for some types of interfaces (e.g. multi-point like) [8]. A common solution to prevent noise amplification due to the above-mentioned redundancy is to apply regularization techniques that only promote the forces that control the most dominant interface dynamics (as, for example, identified using singular value decomposition) [9, 8].

[1] The contribution of individual equivalent force at the interface to the overall assembly response is wrongly estimated.
[2] A useful tool to evaluate if the interface model accounts for all interface DoFs is Interface Completeness Criteria (ICC), see [5].

Recently, as an alternative, various authors introduced the idea of using sparse regression when modeling the interface [10, 11].

The main interest of this study is to provide insights into the implementation and application of the sparse regression for use in inverse problem of TPA methods. LASSO (least absolute shrinkage and selection operator) [12], a regression model for variable selection (shrinkage) of unknown coefficients, is proposed to identify a sparse set of significant interface DoFs from a larger set estimated by the experimentalist in the scope of VPT[3]. Within this study, different aspects of sparse regression when applied to TPA are investigated, such as: accounting for the complex nature of the admittance matrix, normalizing the predictors in the model, effects of over/underdetermination of the inverse problem on the identification of the significant DoFs, grouping of the interface DoFs to retain the physicality of the approach, and frequency-dependent nature of the significant DoFs as a result of sparse regression. The feasibility of the approach is carried out on two case studies that investigate single- and multi-point-like interfaces. The methodology is fully implemented in python using open-source packages.

The paper is organized as follows. In Section 2, a theoretical overview on in-situ TPA and general approaches to interface modeling are given. Section 3 introduces approach to select significant interface DoFs using LASSO. Presented strategy is then validated in Sections 4 and 5 on respective numerical and experimental case studies considering single- and multi-point-like interfaces, respectively. Finally, conclusions are given in Section 5.

2 Background concepts and notations

2.1 In-situ TPA

Consider an assembly of substructures A and B, coupled at the interface, as depicted in Fig. 1a. Substructure A is an active component with the operational excitation $\boldsymbol{f}_1$ acting at node 1. Meanwhile, no excitation force is acting on the passive substructure B. The responses on B are hence a consequence of $\boldsymbol{f}_1$ only, and are observed in three different sets of DoFs: at the interface DoFs ($\boldsymbol{u}_2$), in the proximity of the interface at the indicator DoFs ($\boldsymbol{u}_4$), and away from the interface at the target DoFs ($\boldsymbol{u}_3$).

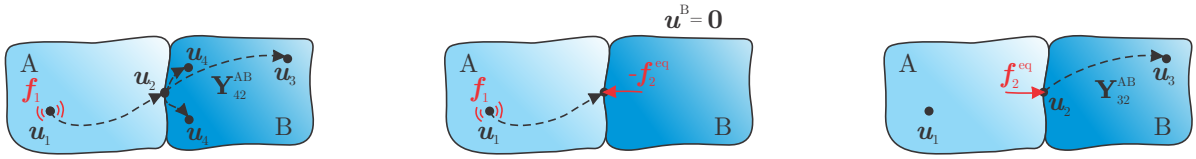

(a) (b) (c)

Figure 1: In-situ TPA: a) assembly of substructures A and B, b) $\boldsymbol{f}_2^{\text{eq}}$ blocking the motion at the interface, c) replicating operational responses with $\boldsymbol{f}_2^{\text{eq}}$.

Source excitations $\boldsymbol{f}_1$ are often not measurable in practice; therefore, in-situ TPA adopts a different approach for describing the operational excitations. A set of equivalent forces $\boldsymbol{f}_2^{\text{eq}}$ is introduced, applied at the interface DoFs. If the source is deactivated, $\boldsymbol{f}_2^{\text{eq}}$ yields the same responses on the passive side $\boldsymbol{u}_3$ as $\boldsymbol{f}_1$. The application of both the operational forces $\boldsymbol{f}_1$ and the equivalent forces $\boldsymbol{f}_2^{\text{eq}}$ acting in the opposite direction simultaneously (Fig. 1b) should therefore remove any response on the passive side. The response at the interface $\boldsymbol{u}_2$ or at the indicator DoFs $\boldsymbol{u}_4$ can be used to calculate the equivalent forces, as follows[4]:

$$\mathbf{0} = \underbrace{\mathbf{Y}^{AB}_{21}\boldsymbol{f}_1}_{\boldsymbol{u}_2} + \mathbf{Y}^{AB}_{22}\left(-\boldsymbol{f}_2^{eq}\right) = \underbrace{\mathbf{Y}^{AB}_{41}\boldsymbol{f}_1}_{\boldsymbol{u}_4} + \mathbf{Y}^{AB}_{42}\left(-\boldsymbol{f}_2^{eq}\right). \tag{1}$$

[3] In this paper, study of sparse regression is limited to the use of VPT within TPA only.

[4] An explicit dependency on the frequency is omitted to improve the readability of the notation, as will be the case for the remainder of the paper.

Expressing the equivalent forces $\boldsymbol{f}_2^{\text{eq}}$ from the indicator responses $\boldsymbol{u}_4$ yields:

$$\boldsymbol{f}_2^{\text{eq}} = \left(\mathbf{Y}_{42}^{\text{AB}}\right)^{+} \boldsymbol{u}_4. \tag{2}$$

The equivalent forces are a valid source description for any passive side [2]. Therefore, they are transferable to an assembly with a modified receiver. Receiver operational responses for the arbitrary assembly (with the same source) can be replicated by the set of equivalent forces (Fig. 1c) as follows:

$$\boldsymbol{u}_3 = \mathbf{Y}_{32}^{\text{AB}} \boldsymbol{f}_2^{\text{eq}}. \tag{3}$$

2.2 Interface modeling

As emphasized earlier, interface modeling is critical to prevent redundancy/bad conditioning or neglecting important transfer paths at the interface. This boils down to accounting for all significant DoFs at the interface.

2.2.1 Equivalent multi-point connection

Using equivalent multi-point connection method (EMPC) for interface modeling, rotational and flexible interface DoFs (such as bending, torsion, etc. [13]) can be implicitly accounted for on the basis of the translational measurements only.

Given that the interface behaves rigidly (Fig. 2), we determine 6 impact locations that are homogeneously distributed in the proximity of the interface, but also distributed in all directions. By exciting these DoFs with impact hammer, we implicitly control all 6 interface DoFs. The same applies for implicitly observing interface DoFs. For the cases of flexible interface behavior, the number of input/outputs DoFs should be adjusted accordingly to avoid neglecting significant transfer paths.

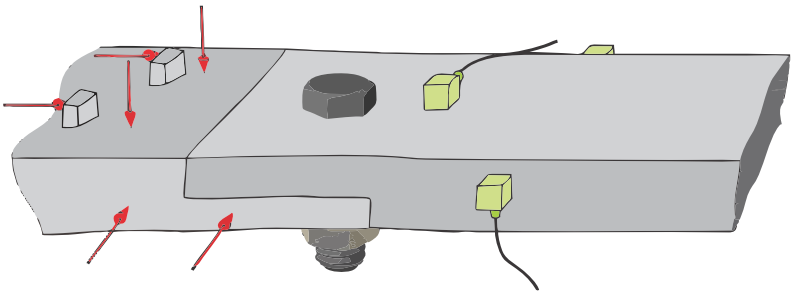

Figure 2: Equivalent multi-point connection.

The approach is simplistic, as no additional geometrical transformation is required to account for rotational or flexible interface DoFs. However, this poses some difficulties when one tries to combine obtained equivalent force set with numerical models for the sake of virtual prototyping [14] or applying the same set of forces to other experimental response models, as the same set of input DoFs must be accessible/obtained for any modified assembly. Also, any discrepancy due to the measurement errors will lead to wrong estimation of individual equivalent force contribution to the overall assembly response.

2.2.2 Virtual point transformation

The theory of the VPT is summarized here according to [6]. The main idea behind the VPT is to choose a virtual point (VP) near the physical interface of the interface[5] and obtain FRFs for n_{u} responses $\boldsymbol{u}$ and

[5]Exact position of virtual point is known to the experimentalist and can be obtained for any assembly regardless of how interface is accessible to measurement equipment. Although different inputs are used for source characterization on different assemblies, virtual point can always be placed exactly the same.

n_f excitations $\boldsymbol{f}$ in the proximity of this point ($\mathbf{Y}_\mathrm{uf} \in \mathbb{C}^{n_\mathrm{u} \times n_\mathrm{f}}$). $\mathbf{Y}_\mathrm{uf}$ is then projected onto the interface deformation modes (IDMs). If we assume only the rigid-body IDMs (rigid interface behavior) then the virtual point has $m = 6$ DoFs, i.e., three translational and three rotational DoFs. In addition, flexible IDMs can also be considered to describe a more complex interface behavior [13]. The transformation is achieved using the following equation:

$$\mathbf{Y}_\mathrm{qm} = \mathbf{T}_\mathrm{u} \mathbf{Y}_\mathrm{uf} \mathbf{T}_\mathrm{f}^\mathrm{T}, \tag{4}$$

where $\mathbf{T}_\mathrm{u}$ is the displacement transformation matrix and $\mathbf{T}_\mathrm{f}$ is the force transformation matrix. $\mathbf{Y}_\mathrm{qm} \in \mathbb{C}^{m \times m}$ is the VP FRF matrix with a perfectly collocated input and output DoFs. It is advisable that the number of measured responses and excitations, i.e., n_u and n_f, respectively, exceed the dimensions of the VP FRF matrix, $m \times m$ [6].

The kinematic relation between m responses at the virtual point $\boldsymbol{q}$ and n_u sensor displacements $\boldsymbol{u}$ can be written as:

$$\boldsymbol{u} = \mathbf{R}_\mathrm{u} \boldsymbol{q}. \tag{5}$$

The IDMs are contained in $\mathbf{R}_\mathrm{u} \in \mathbb{R}^{n_\mathrm{u} \times m}$, which is a non-square matrix that provides the sensor locations and orientations with respect to the VP (Fig. 3). For more information about the assembly of the $\mathbf{R}_\mathrm{u}$ the

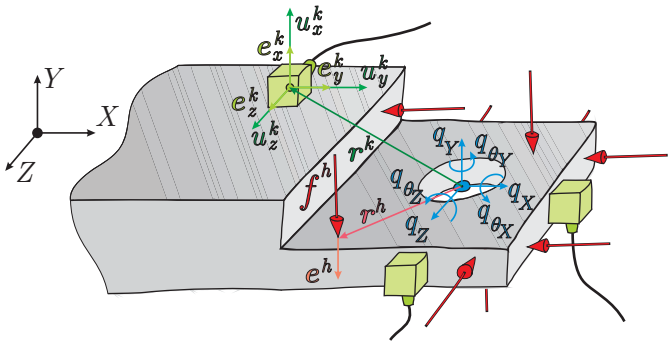

Figure 3: Projection of responses on the k-th triaxial accelerometer and the h-th excitation onto the virtual point[6].

reader is referred to [6]. Solving Eq. (5) for $\boldsymbol{q}$ in a least-square sense yields the displacements of the VP:

$$\boldsymbol{q} = \left(\mathbf{R}_\mathrm{u}^\mathrm{T} \mathbf{R}_\mathrm{u}\right)^{-1} \mathbf{R}_\mathrm{u}^\mathrm{T} \boldsymbol{u} = \mathbf{T}_\mathrm{u} \boldsymbol{u} \quad \Rightarrow \quad \mathbf{T}_\mathrm{u} = \left(\mathbf{R}_\mathrm{u}^\mathrm{T} \mathbf{R}_\mathrm{u}\right)^{-1} \mathbf{R}_\mathrm{u}^\mathrm{T}. \tag{6}$$

Similarly, the loads $\boldsymbol{m}$ at the virtual point are obtained for a given vector of forces $\boldsymbol{f}$ in the proximity of the VP. The contribution from all the input forces can be combined and expressed as follows:

$$\boldsymbol{m} = \mathbf{R}_\mathrm{f}^\mathrm{T} \boldsymbol{f}, \tag{7}$$

where the IDM matrix $\mathbf{R}_\mathrm{f}^\mathrm{T} \in \mathbb{R}^{m \times n_\mathrm{f}}$ contains the positions and orientations for all the excitation locations with respect to the VP (Fig. 3). A more detailed description of $\mathbf{R}_\mathrm{f}$ is given in [6]. The inverse relationship of Eq. (7) is derived with a constrained minimization for forces:

$$\boldsymbol{f} = \mathbf{R}_\mathrm{f} \left(\mathbf{R}_\mathrm{f}^\mathrm{T} \mathbf{R}_\mathrm{f}\right)^{-1} \boldsymbol{m} = \mathbf{T}_\mathrm{f}^\mathrm{T} \boldsymbol{m} \quad \Rightarrow \quad \mathbf{T}_\mathrm{f}^\mathrm{T} = \mathbf{R}_\mathrm{f} \left(\mathbf{R}_\mathrm{f}^\mathrm{T} \mathbf{R}_\mathrm{f}\right)^{-1}. \tag{8}$$

With respect to the in-situ TPA (Eq. (2)), no transformation of the displacement is necessary, only of the forces. Hence transfer path admittance in Eqs. (2) and (3) can be expressed as follows with regards to the

[6]The position vector from the VP to the center of the sensor is denoted by $\boldsymbol{r}^k$. The unit vector for each accelerometer axis is $\boldsymbol{e}_i^k$ and the response in each axis is denoted by u_i^k ($i \in (x, y, z)$). The position vector from VP to the force impact is $\boldsymbol{r}^h$, the impact direction is $\boldsymbol{e}^h$ and the impact magnitude is f^h.

VPT[7]:

$$\mathbf{Y}_{42}^{\mathrm{AB}} = \mathbf{Y}_{4\mathrm{f}}^{\mathrm{AB}}\,\mathbf{T}_{\mathrm{f}}^{\mathrm{T}}, \tag{9}$$

$$\mathbf{Y}_{32}^{\mathrm{AB}} = \mathbf{Y}_{3\mathrm{f}}^{\mathrm{AB}}\,\mathbf{T}_{\mathrm{f}}^{\mathrm{T}}. \tag{10}$$

Commonly, a reduction using a geometrical basis is built by means of rigid IDMs only. That means the transfer through flexible interface DoFs is neglected, thus limiting the approach for interfaces that only behave rigidly. In order to overcome this issue, two methodologies may be adopted:

- Use of additional non-collocated virtual points that can approximate flexible interface motion by piecewise rigid interface regions and hence implicitly account for flexible interface DoFs.
- Including flexible IDMs in the defined reduction bases $\mathbf{R}_{\mathrm{u}}$ and $\mathbf{R}_{\mathrm{f}}$ that are defined from the relative location of the measurement position with respect to the virtual point [13, 15]. However, the manual selection of flexible IDMs included in the reduction spaces is a case-specific cumbersome task that often relies on user-judgment.

Note that all approaches require considerable measurement effort in order to ensure sufficient over/underdetermination of the output/input transformations. Furthermore, all approaches are sensitive to bias errors in input/output position/direction, although this can be identified to some extent by measurement quality indicators [6].

3 LASSO for admittance-based TPA within VPT framework

As described above, using VPT for interface modeling proves to be beneficial for source characterization but requires manual selection of interface DoFs which often leads to redundancy issues. Within this section, the use of LASSO is introduced to identify significant IDMs from the (redundant) IDM set proposed by the experimentalist. Compared to the already established approach in [11], where LASSO is applied to obtain a sparse set of equivalent forces directly within the inverse problem (Eq. (2)), here it merely serves to suggest the number and type of the IDMs that should be kept in the VPT to avoid redundancy and amplification of equivalent force noise.

In other words, looking back to the problem (inverse relation of Eq. (9)):

$$\mathbf{Y}_{4\mathrm{f}}^{\mathrm{AB}} = \mathbf{Y}_{42}^{\mathrm{AB}}\,\mathbf{R}_{\mathrm{f}}^{\mathrm{T}}, \tag{11}$$

we are trying to find which dynamic information in $\mathbf{R}_{\mathrm{f}}$ (which columns or IDMs) would be important to eventually find a good approximation of $\boldsymbol{u}_4$ due to $\boldsymbol{f}_2^{\mathrm{eq}}$, related by $\mathbf{Y}_{42}^{\mathrm{AB}}$ (Eq. (2)).

First, we separate VPT (Eq. (11)) for real and imaginary parts respectively:

$$\begin{bmatrix}\Re\left(\mathbf{Y}_{4\mathrm{f}}^{\mathrm{AB}}\right) & \Im\left(\mathbf{Y}_{4\mathrm{f}}^{\mathrm{AB}}\right)\end{bmatrix} = \begin{bmatrix}\Re\left(\mathbf{Y}_{42}^{\mathrm{AB}}\right) & \Im\left(\mathbf{Y}_{42}^{\mathrm{AB}}\right)\end{bmatrix}\begin{bmatrix}\mathbf{R}_{\mathrm{f}}^{\mathrm{T}} & \mathbf{0}\\ \mathbf{0} & \mathbf{R}_{\mathrm{f}}^{\mathrm{T}}\end{bmatrix} \tag{12}$$

and then vectorize column-wise [16] to obtain[8]:

[7] Distinction in notation should be emphasized at this point which is adopted for the remainder of the paper: input subscript $(\star)_{\mathrm{f}}$ relates to the input DoFs characterized directly with the measurement campaign, while input subscript $(\star)_2$ relates to the virtual input DoFs.

[8] $\boldsymbol{Y}_{4\mathrm{f}_1}^{\mathrm{AB}}$ is the full column of the admittance matrix $\mathbf{Y}_{4\mathrm{f}}^{\mathrm{AB}}$ for the first excited input DoF etc.

$$\begin{bmatrix} \Re\left(\boldsymbol{Y}_{4\mathrm{f}_1}^{\mathrm{AB}}\right) \\ \Re\left(\boldsymbol{Y}_{4\mathrm{f}_2}^{\mathrm{AB}}\right) \\ \vdots \\ \Im\left(\boldsymbol{Y}_{4\mathrm{f}_1}^{\mathrm{AB}}\right) \\ \Im\left(\boldsymbol{Y}_{4\mathrm{f}_2}^{\mathrm{AB}}\right) \end{bmatrix} = \left[\begin{bmatrix} \mathbf{R}_{\mathrm{f}} & \mathbf{0} \\ \mathbf{0} & \mathbf{R}_{\mathrm{f}} \end{bmatrix} \otimes \mathbf{I} \right] \begin{bmatrix} \Re\left(\boldsymbol{Y}_{42_1}^{\mathrm{AB}}\right) \\ \Re\left(\boldsymbol{Y}_{42_2}^{\mathrm{AB}}\right) \\ \vdots \\ \Im\left(\boldsymbol{Y}_{42_1}^{\mathrm{AB}}\right) \\ \Im\left(\boldsymbol{Y}_{42_2}^{\mathrm{AB}}\right) \end{bmatrix} \tag{13}$$

or:

$$\boldsymbol{y} = \mathbf{A}\,\boldsymbol{x}, \tag{14}$$

where $\mathbf{A}$ is the coefficient matrix and $\boldsymbol{y}$ is the vector of constant terms. LASSO sets to find the $\boldsymbol{x}$ that minimizes:

$$||\mathbf{A}\,\boldsymbol{x} - \boldsymbol{y}||_2^2 + \alpha\,||\boldsymbol{x}||_1, \tag{15}$$

where $||\boldsymbol{x}||_1$ is the sum of the absolute vector values and α is the regularization parameter that controls the strength of the penalty. By penalizing the absolute values of the coefficients, LASSO encourages many coefficients to be exactly zero. This leads to sparse solutions, effectively performing feature selection by identifying the most important features. Sparsity constraint means that there isn't a closed form solution to the problem and optimization algorithms must be used to estimate $\boldsymbol{x}$. The algorithm used to fit the model in this work is coordinate descent [17]. It iteratively updates the coefficients to minimize the objective function, adjusting the balance between fitting the data and keeping the coefficients small. The best model is selected by cross-validation [17].

The following properties of the VPT must also be accounted for when performing sparse regression:

1. Real and imaginary parts of admittance matrix should both be either existent or zero in the solution proposed by the LASSO[9]. Implementation of group LASSO [18] should be applied for this reason where real and imaginary parts related to the same VP DoF are given the same grouping number.

2. Another question arises whether or not columns of the VP admittance in the solution proposed by the LASSO should be sparse. This sparsity means that the interface DoF is not observable at all indicator DoFs and will have zero contribution to the response at these DoFs which is (probably) not the case in reality. Hence it would make sense to enforce the columns to be either fully-existent or fully-zero in the solution. Again, group LASSO can be applied to achieve that. However, IDM grouping enforces a stringent constraint by promoting group-wise sparsity, leading to the inclusion of some IDMs with marginal importance. At various point in this paper, significant IDMs are identified either with or without IDM grouping, and benefits of each approach are discussed.

3. Because different (translational, rotational and flexible) IDMs are on different "scales", IDMs with larger scales are penalized less by the LASSO and the model may favor them, leading to suboptimal selection of significant interface DoFs. Normalization should be applied before fitting a LASSO regression in order to properly estimate the significance of different IDMs (so that each IDM has a consistent "power", making the model more interpretable). In this study, each column of $\mathbf{A}$ was scaled by its maximum absolute value [17].

4. Frequency-dependent nature of the transformation can lead to different interface DoFs being significant for individual frequency lines. Frequency-dependent transformation can thus be performed for characterization of the source, but that means the type of interface DoFs varies throughout the frequency range of interest. A simple (constant) interface DoF selection can be performed by the user

[9] In other words, if a real part of a single FRF at selected frequency is equal to zero in the solution proposed by LASSO, imaginary part should also be equal to zero.

by inspecting which interface DoFs appear most often in the sparse solution across entire frequency range, treating them as a significant set. As an alternative, multi task LASSO [17] can be applied to enforce that the same interface DoFs are selected across entire frequency range of interest. In order to respect the grouping of real and imaginary parts of the FRFs, multi task LASSO is implemented in a following manner. Similar to Eq. (12), VPT is done separately for the real and imaginary parts, however, we also separate vectorization as:

$$\begin{bmatrix} \Re\left(\boldsymbol{Y}_{4\mathrm{f}_1}^{\mathrm{AB}}\right) \\ \Re\left(\boldsymbol{Y}_{4\mathrm{f}_2}^{\mathrm{AB}}\right) \\ \vdots \end{bmatrix} = [\mathbf{R}_\mathrm{f} \otimes \mathbf{I}] \begin{bmatrix} \Re\left(\boldsymbol{Y}_{42_1}^{\mathrm{AB}}\right) \\ \Re\left(\boldsymbol{Y}_{42_2}^{\mathrm{AB}}\right) \\ \vdots \end{bmatrix}, \tag{16}$$

$$\begin{bmatrix} \Im\left(\boldsymbol{Y}_{4\mathrm{f}_1}^{\mathrm{AB}}\right) \\ \Im\left(\boldsymbol{Y}_{4\mathrm{f}_2}^{\mathrm{AB}}\right) \\ \vdots \end{bmatrix} = [\mathbf{R}_\mathrm{f} \otimes \mathbf{I}] \begin{bmatrix} \Im\left(\boldsymbol{Y}_{42_1}^{\mathrm{AB}}\right) \\ \Im\left(\boldsymbol{Y}_{42_2}^{\mathrm{AB}}\right) \\ \vdots \end{bmatrix}. \tag{17}$$

Eqs. (16) and (17) are then stacked together with respect to the frequency dimension (i.e. depth-wise). In this manner, equal sparsity is obtained for real and imaginary parts. Note that IDM grouping is neglected in this case.

Possible ways to identify significant IDMs from the sparse solution are demonstrated in Sections 4 and 5.

In this study, VPT implementation as a part of open-source python package pyFBS was used [19], while (group and multi task) LASSO is implemented using an open-source python packages scikit-learn [17] and celer [20].

4 Numerical study

Numerical study deals with an assembly where connectivity between active and passive side is ensured through single-point-like interface that behaves rather rigidly in the frequency range of interest. Similar interface types are commonly modeled using a single virtual point considering rigid IDMs only. The goal of the first study is to establish whether or not LASSO is able to recognize the significance of translational and rotational interface DoFs only.

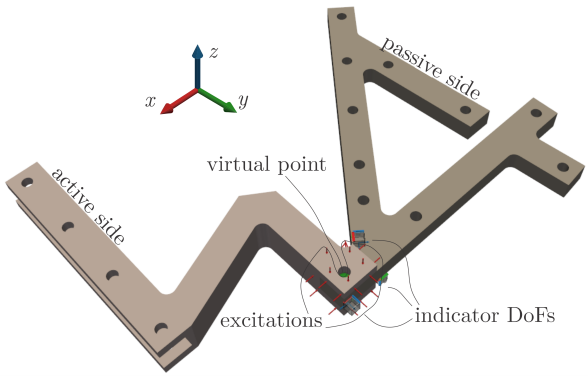

Figure 4: Assembly used in numerical case study.

Structure of interest[10] is presented in Fig. 4. Active and passive side of the assembly share a relatively small contact area and are perfectly bonded at the interface. The material properties for both analyzed structures are presented in Table 1. Assembly is subjected to free boundary conditions.

[10]CAD models for all substructures considered in this study are freely available at the pyFBS repository [19].

Table 1: Beam-like structure's material properties.

Parameter	Unit	Value
ρ	kg/m^3	2750
E	GPa	70

The measurement setup was simulated. 30 impact positions were selected in the proximity of the interface at the active side of the assembly. These impact positions were equally distributed over the interface and between all the directions to maximize the interface controllability. Nine response locations were selected in the vicinity of the interface on the passive side (indicator DoFs). FRFs relating motion at the indicator DoFs to the excitations close to the interface ($\mathbf{Y}_{4f}^{\mathrm{AB}}$) were calculated in the frequency range of interest 0 - 2000 Hz with a frequency resolution of 2 Hz. To make the subsequent analysis a little more realistic, random measurement errors were simulated. A Gaussian random distributed noise was added to the real and imaginary parts of each FRF frequency by frequency.

Due to the use of a single-point connection type, an assumption of rigid interface behavior is adopted in the following. To validate this assumption, singular value decomposition (SVD, [21]) was performed on $\mathbf{Y}_{4f}^{\mathrm{AB}}$ which serves as a quick assessment of the number of interface DoFs. By inspecting the magnitude of the obtained singular values (SVs) (Fig. 5a) and the ratio between the sum of the first six SVs and the sum of all SVs (Fig. 5b), it is evident that interface dynamics can be characterized by 6 DoFs (i.e. 3 rigid translations and 3 rigid rotations).

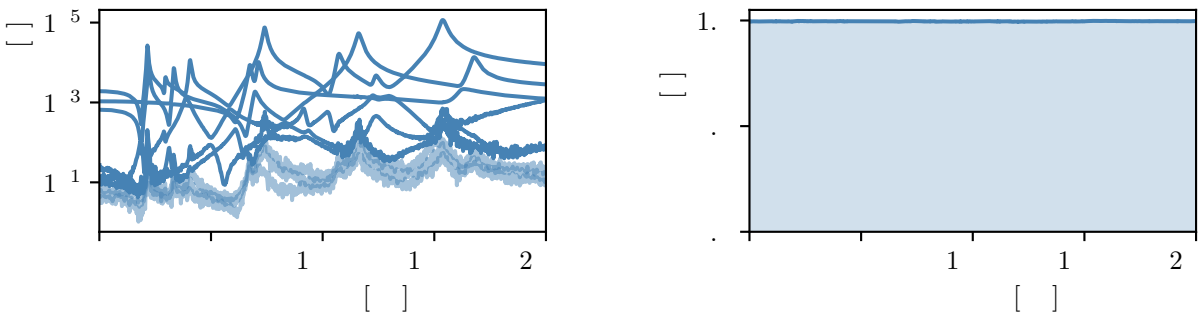

(a) (b)

Figure 5: Significant interface DoF selection for assembly used in numerical study: a) singular values of $\mathbf{Y}_{42}^{\mathrm{AB}}$, b) ratio of the sum of the first 6 singular values and sum of all singular values.

A single virtual point was selected to model the interface between active and passive side. The methodology presented in Section 3 was applied to estimate the significant IDMs used for modeling the interface. Grouping was applied to pair real and imaginary parts of the FRFs as well as the individual IDMs. Initially, all possible IDMs (besides rigid IDMs, simple extension, torsion, skewing and bending modes are included in the VP model [13]) are considered in the $\mathbf{R}_{\mathrm{f}}$ matrix (Eq. (12)), for which LASSO is then applied to identify a set of significant IDMs. Initially, identification is performed per individual frequency line. Results for each frequency line are then added together to identify IDMs with highest repetition per frequency score. Given that the problem is overdetermined (30 impacts are to be transformed into the VP with 24 DoFs), IDM repetition is presented in Fig. 6.

Based on the barchart presented in Fig. 6, one should use only rigid IDMs to model the interface of the structure of interest using a single VP, while adding additional IDMs to the transformation (even in the case with excess of impacts) would only lead to redundancy issues.

In the following, the robustness of the proposed approach is investigated in cases where the experimentalist cannot ensure that the number of measured inputs exceeds the number of IDMs considered (i.e., whether

[11] f_i represents translational interface forces, m_i represents moments, e_i represents extension forces, t_i represents torsional forces, $s_{i,j}$ represents skewing forces and b_{ij} represents bending forces for $i,\ j\ \in \{x,\ y,\ z\}$ (coordinate axes).

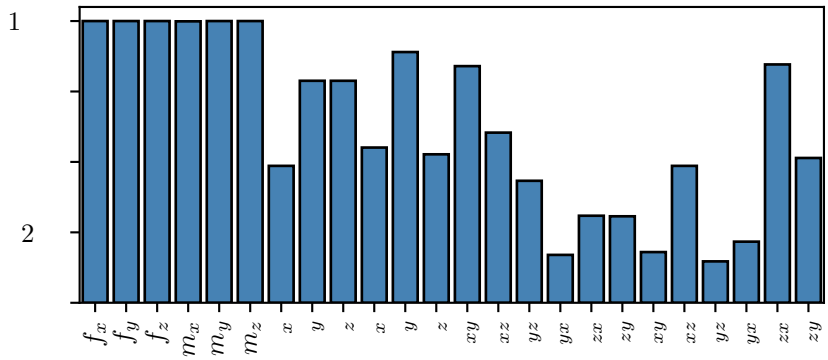

Figure 6: IDM significance for the numerical study considering the VPT is overdetermined. For 1000 frequency lines, rigid IDMs were identified as significant at each one[11].

the solution obtained by LASSO is also meaningful for determined and underdetermined problems). Hence next scenario investigates the consistency of IDM estimation if the problem fed to LASSO is determined (i.e. 24 impacts are to be transformed into the VP with 24 DoFs). For this example, 6 inputs of the admittance matrix $\mathbf{Y}_{4f}^{\mathrm{AB}}$ were neglected. Results are presented in Fig. 7 and, similarly to Fig. 6, show that rigid IDMs are deemed suitable to model the interface between active and passive side.

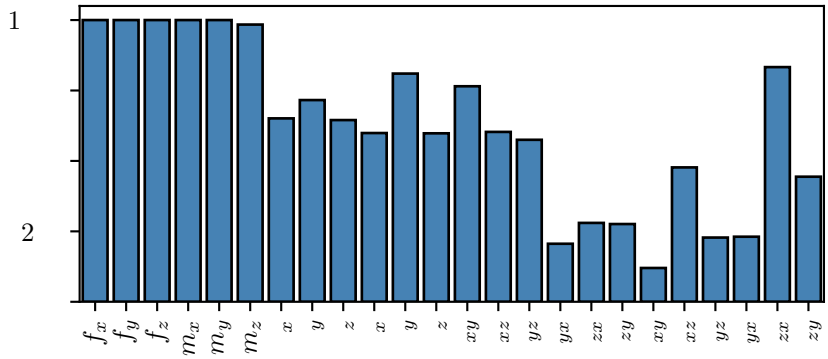

Figure 7: IDM significance for the numerical study considering the VPT is determined. For 1000 frequency lines, rigid IDMs were identified as significant at each one.

Next, the number of inputs was reduced so the problem fed to LASSO was underdetermined (i.e. 9 impacts, as commonly measured for VP with rigid DoFs, are to be transformed into the VP with 24 DoFs). Results are presented in Fig. 8 are clearly not consistent with rigid interface assumption, thus limiting the implementation to (over) determined problems only.

To avoid the selection of significant IDMs over individual frequency lines, multi task LASSO was applied in the final part of this numerical study to enforce the same interface DoFs are selected across entire frequency range of interest. Multi task LASSO was implemented in a way that real and imaginary parts of the FRFs appear as pairs in the solution while IDM grouping constrain was lifted in this case. Only the determined problem was considered. Results are presented in the Fig. 9. Again, rigid IDMs can be recognized as significant. Furthermore, the importance of the contribution for the flexible IDMs can be judged more clearly due to the lifted IDM grouping constrain.

To summarize, given that the problem fed to LASSO is (over)determined, the methodology promises to be useful for identifying the number and type of the significant interface DoF to be included in the interface model using VPT. This claim is further validated on the experimental study.

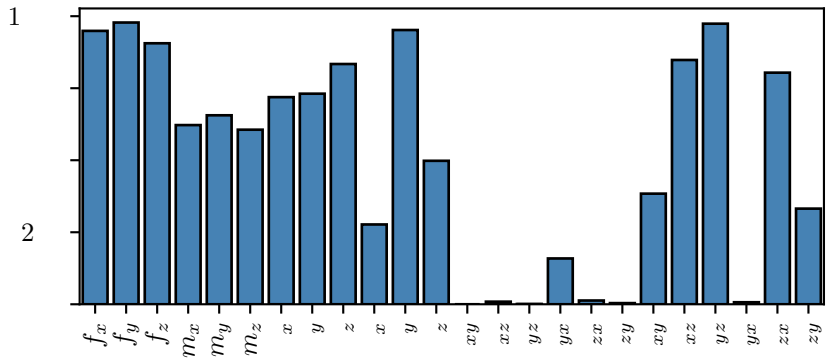

Figure 8: IDM significance for the numerical study considering the VPT is underdetermined.

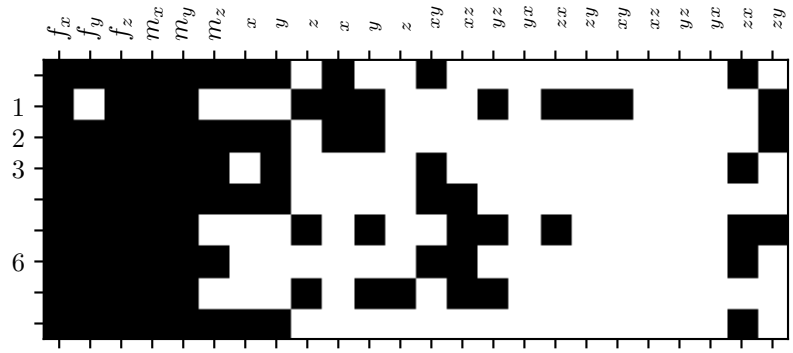

Figure 9: Result of multi task LASSO. Black squares indicate suitable subset selection and the significant IDMs can be identified based on their column-wise repeatability.

5 Experimental study

Experimental study investigates a case where multi-point-like interface is used to assemble active and passive substructures. Interface model for similar assemblies often leads to redundancy of the modeled interface DoFs (for instance if the experimentalist models each connection point with 6 DoFs). This is commonly resolved using regularization techniques. Sparse regression approach is applied in this case to recognize the number and type of significant interface DoFs to characterize the source.

The test structure is designed to mimic the dynamics in a real car of an engine unit flexibly mounted on a chassis (Fig. 10). Rubber mounts from the automotive industry are mounted on a dedicated frame and are used to suspend a steel plate representing the source substructure. The structure is intended as a laboratory test bench for an application of different concepts of dynamic substructuring and transfer path analysis [22].

Each rubber mount was equipped with three (nine in total) triaxial modal accelerometers Kistler Type 8688A which acted as indicator DoFs. Additionally, two accelerometers of the same type were mounted to the frame substructure away from the interface, which acted as target DoFs. In the proximity of the three mounting points at the source, 27 impact positions were determined (9 per connection point). In this manner, all interface DoFs are properly controlled and observed, and source is characterized independently of the rubber mounts. All the FRFs were measured by impact testing using a modal hammer with a vinyl tip. Operational excitation was once again simulated using impact excitation at the internal DoF of the source.

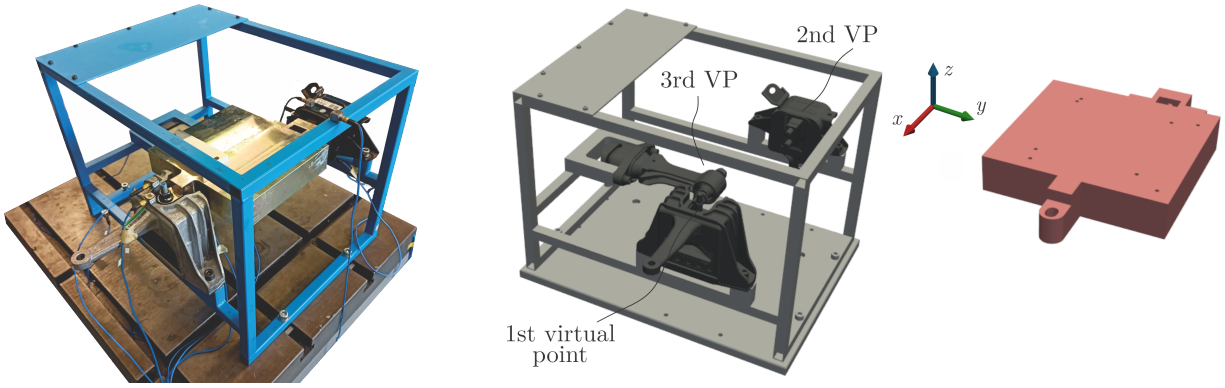

(a) (b) (c)

Figure 10: Experimental study on multi-point-like interface: a) automotive testbench, b) receiver (frame in gray and rubber mounts in black) mounted to the approximately rigid ground, c) source.

Five sets of equivalent forces were estimated:

- **set 1:** The interface is modeled using the equivalent multi-point connection approach. In this case, equivalent forces are estimated at all 27 input DoFs in the proximity of the interface at the source.
- **set 2:** The interface is modeled using the equivalent multi-point connection approach using regularized admittance matrix $\mathbf{Y}_{4f}^{AB}$. Truncated singular value decomposition was applied by discarding the lowest 18 SVs, based on their magnitude.
- **set 3:** The interface is modeled using three virtual points (at each connection point with the rubber mounts, see Fig. 10b) with 6 rigid DoFs per VP. In this case, equivalent forces are estimated at 18 virtual input DoFs.
- **set 4:** The interface is modeled using three virtual points using regularized admittance matrix $\mathbf{Y}_{42}^{AB}$. Truncated singular value decomposition was applied by discarding the lowest 9 SVs, based on their magnitude.
- **set 5:** The interface is modeled using virtual DoFs proposed by LASSO implementation, presented in the following.
- **set 6:** The interface is modelled using virtual DoFs proposed by LASSO with additional regularization applied (smallest two singular values were discarded).

The methodology presented in Section 3, specifically multi task LASSO, was applied to estimate the significant IDMs used for modeling the interface in sets 5 & 6. This implementation was selected as the use of grouping LASSO was found to be too stringent when promoting IDM group-wise sparsity. Results are presented in Fig. 11. This led to selection of the significant interface DoFs used in sets 5 & 6, i.e. $1-f_x$, $1-f_y$, $1-f_z$, $2-f_x$, $2-f_y$, $2-f_z$, $2-m_z$, $3-f_x$, $3-f_y$, $3-f_z$ and $3-m_z$.

After all 6 sets of equivalent were estimated on the initial assembly, the latter was modified by replacing the used soft rubber mounts for significantly stiffer ones. The new (modified) assembly was used to evaluate the transferability of the estimated equivalent force sets. The same operational excitation[12] was applied at the source, while the response at the target DoFs away from the interface was measured. This was treated as a reference response. To predict the response from the equivalent forces (Eq. (3)), the admittance matrix of the modified assembly relating the excitation at the interface and response at the target DoFs ($\mathbf{Y}_{32}^{AB}$) was measured. Depending on the equivalent force set used, $\mathbf{Y}_{32}^{AB}$ was transformed to the virtual DoFs set to ensure the collocation between $\mathbf{Y}_{32}^{AB}$ and $\boldsymbol{f}_2^{eq}$ (for sets 3-6).

[12]Exactly the same operating excitation had to be applied to the active side of the modified assembly to retain the validity of the equivalent forces, which is challenging to achieve using impact hammer and excitation by hand. In order to sufficiently replicate the operational excitation from the initial assembly, the admittance of the novel assembly relating response DoFs and operational impact positions was measured first. Then, the impact signal at operational impact positions from the initial assembly was multiplied by the admittance of the novel assembly to obtain the operational responses at the modified passive side for the same operating excitation.

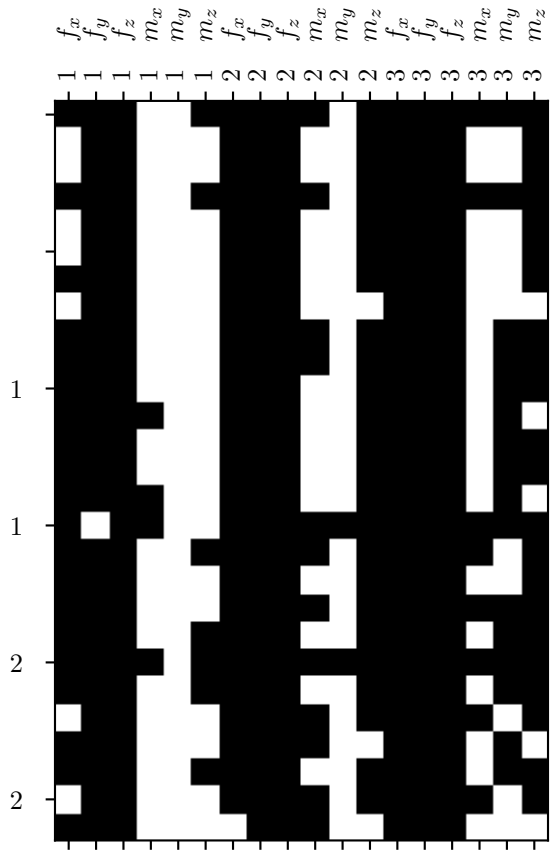

Figure 11: Result of multi task LASSO for case study considering multi-point interface (1 - 1st virtual point, 2 - 2nd virtual point, 3 - 3rd virtual point).

Response predictions from cross validation for all 6 equivalent force sets are presented in Fig. 12. Fig. 12a presents results without applied regularization. It is evident that the redundancy of the interface DoFs in the case of EMPC interface model causes high error magnification in the predicted response. The agreement between reference and prediction is significantly higher given the virtual DoFs are used to model the interface. Here, using interface DoFs based on LASSO suggestion slightly outperforms interface model with 18 virtual DoFs (set 3).

Fig. 12b presents response prediction given the regularization is applied to minimize the contribution of the equivalent force noise in the solution. In this case, responses from all three approaches match closely with the reference, and no major discrepancies from any approach are present.

The agreement between the reference and the predictions is additionally investigated using coherence criteria [6]. Fig.13 shows the highest agreement between the reference and the prediction without applied regularization is obtained given the interface model based on the LASSO suggestion. Given the solution is regularized properly, minor differences in response prediction are again observed from all three approaches.

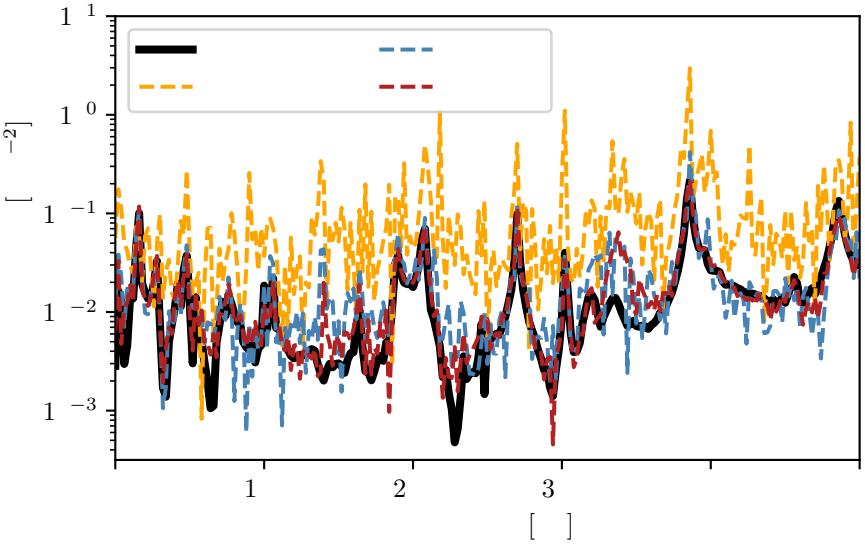

(a)

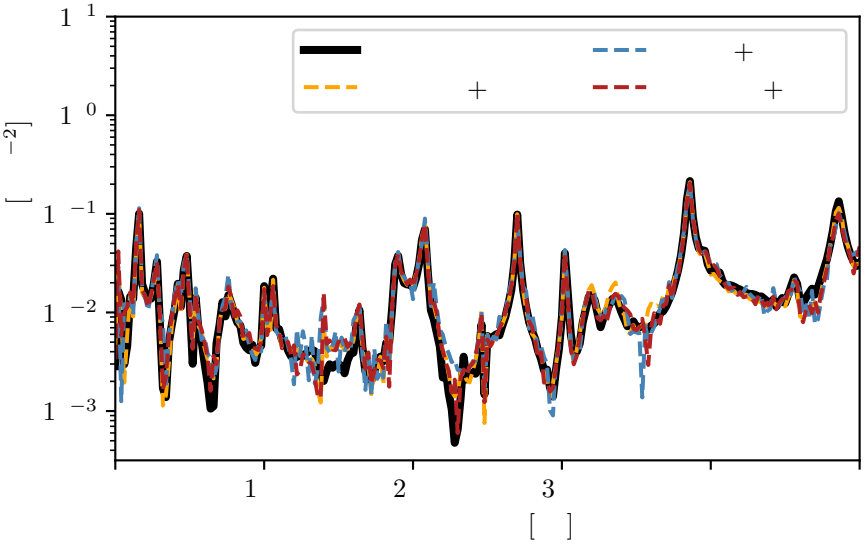

(b)

Figure 12: Cross validation of the equivalent force sets from different interface models: a) without using regularization, b) using regularization.

6 Conclusions

This paper utilizes sparse regression approach to the identification of significant interface DoFs when modeling the interface in the scope of admittance-based transfer path analysis. The aim of the proposed approach is to reduce ill-conditioning of the inverse TPA problem which arises due to redundancy of the interface DoFs estimated by the experimentalist. By reducing measurement error propagation to the estimated set of forces representing the vibrating source, this method serves as an alternative to traditional regularization techniques.

The regression model LASSO (least absolute shrinkage and selection operator) is implemented within a virtual point framework to identify significant virtual interface DoFs. Rather than directly obtaining a sparse set of equivalent forces, this approach merely suggests which virtual DoFs should be retained for modeling the interface. The final selection of interface DoFs remains at the discretion of the experimentalist, who may also apply additional regularization techniques if necessary when obtaining equivalent force set. The

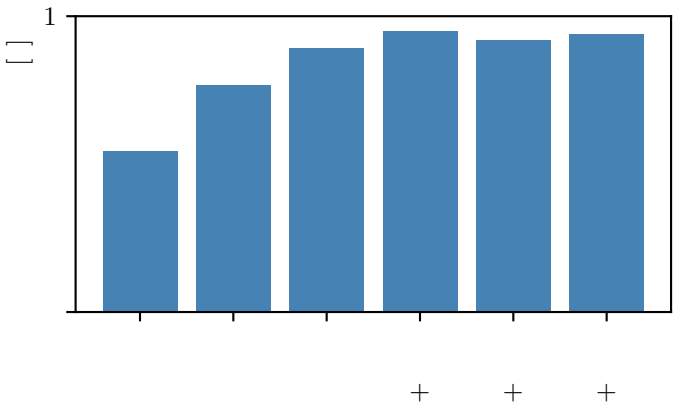

Figure 13: Cross validation of the equivalent force sets from different interface models using coherence criteria.

paper discusses the performance of two LASSO extensions, namely group LASSO and multi-task LASSO. The implementation considers the complex nature of the FRFs by pairing the real and imaginary parts in the solution, normalizing the predictors to avoid bias due to differing scales of the DoF types (i.e. translational, rotational, etc.), and accounting for the frequency-dependent nature of the transformation so that DoF selection is performed over the entire frequency range of interest.

Numerical and experimental case studies are presented to demonstrate the feasibility of the proposed approach, with results comparable to established techniques for robustly estimating the equivalent force set.

References

[1] J. W. Verheij, "Multi-path sound transfer from resiliently mounted shipboard machinery: Experimental methods for analyzing and improving noise control," 1982.

[2] M. V. van der Seijs, D. De Klerk, and D. J. Rixen, "General framework for transfer path analysis: History, theory and classification of techniques," *Mechanical Systems and Signal Processing*, vol. 68, pp. 217–244, 2016.

[3] A. Moorhouse, A. Elliott, and T. Evans, "In situ measurement of the blocked force of structure-borne sound sources," *Journal of sound and vibration*, vol. 325, no. 4-5, pp. 679–685, 2009.

[4] M. Wernsen, M. Van Der Seijs, and D. de Klerk, "An indicator sensor criterion for in-situ characterisation of source vibrations," in *Sensors and Instrumentation, Volume 5: Proceedings of the 35th IMAC, A Conference and Exposition on Structural Dynamics 2017*. Springer, 2017, pp. 55–69.

[5] J. Meggitt and A. Moorhouse, "On the completeness of interface descriptions and the consistency of blocked forces obtained in situ," *Mechanical Systems and Signal Processing*, vol. 145, p. 106850, 2020.

[6] M. V. van der Seijs, D. D. van den Bosch, D. J. Rixen, and D. de Klerk, "An improved methodology for the virtual point transformation of measured frequency response functions in dynamic substructuring," in *4th ECCOMAS thematic conference on computational methods in structural dynamics and earthquake engineering*, vol. 4, 2013.

[7] M. Haeussler, T. Mueller, E. Pasma, J. Freund, O. Westphal, and T. Voehringer, "Component tpa: Benefit of including rotational degrees of freedom and over-determination," in *Proceedings of the international conference on noise and vibration engineering, Leuven, Belgium*, 2020, pp. 7–9.

[8] D. Ocepek, F. Trainotti, G. Čepon, D. J. Rixen, and M. Boltežar, "Different displacement reduction spaces for the use in admittance-based tpa methods," in *IMAC XLII*, 2024.

[9] M. Häußler, "Modular sound & vibration engineering by substructuring," Ph.D. dissertation, Technische Universität München, 2021.

[10] VIBES.technology. Patent pending! x-dof improves your blocked forces. [Online]. Available: https://www.vibestechnology.com/news/xdof/

[11] S. Carter, "Thoughts on using sparse inverse solutions in transfer path analysis," in *IMAC XLII*, 2024.

[12] R. Tibshirani, "Regression shrinkage and selection via the lasso," *Journal of the Royal Statistical Society Series B: Statistical Methodology*, vol. 58, no. 1, pp. 267–288, 1996.

[13] E. Pasma, M. v. d. Seijs, S. Klaassen, and M. v. d. Kooij, "Frequency based substructuring with the virtual point transformation, flexible interface modes and a transmission simulator," in *Dynamics of Coupled Structures, Volume 4: Proceedings of the 36th IMAC, A Conference and Exposition on Structural Dynamics 2018*. Springer, 2018, pp. 205–213.

[14] A. Moorhouse, A. Elliott, and J. Meggitt, "Virtual acoustic prototyping-a story of four decades."

[15] J. O. Almirón, F. Bianciardi, and W. Desmet, "Flexible interface models for force/displacement field reconstruction applications," *Journal of Sound and Vibration*, vol. 534, p. 117001, 2022.

[16] F. R. Kschischang. (2022) Kronecker product and vectorization. [Online]. Available: https://www.comm.utoronto.ca/~frank/notes/vec.pdf

[17] F. Pedregosa, G. Varoquaux, A. Gramfort, V. Michel, B. Thirion, O. Grisel, M. Blondel, P. Prettenhofer, R. Weiss, V. Dubourg *et al.*, "Scikit-learn: Machine learning in python," *the Journal of machine Learning research*, vol. 12, pp. 2825–2830, 2011.

[18] M. Yuan and Y. Lin, "Model selection and estimation in regression with grouped variables," *Journal of the Royal Statistical Society Series B: Statistical Methodology*, vol. 68, no. 1, pp. 49–67, 2006.

[19] T. Bregar, A. El Mahmoudi, M. Kodrič, D. Ocepek, F. Trainotti, M. Pogačar, M. Göldeli, G. Čepon, M. Boltežar, and D. J. Rixen, "pyfbs: A python package for frequency based substructuring," *Journal of Open Source Software*, vol. 7, no. 69, p. 3399, 2022.

[20] M. Massias, A. Gramfort, and J. Salmon, "Celer: a fast solver for the lasso with dual extrapolation," in *Proceedings of the 35th International Conference on Machine Learning*, vol. 80, 2018, pp. 3321–3330.

[21] G. Strang, *Computational science and engineering*, 2007.

[22] A. El Mahmoudi, F. Trainotti, K. Park, and D. Rixen, "In-situ tpa for nvh analysis of powertrains: an evaluation on an experimental test setup," in *AAC 2019: Aachen Acoustics Colloquium/Aachener Akustik Kolloquium*, 2019.